

Incommensurate spin excitations stabilized multiferroic phase in CuO

Guangxi Jin,¹ Kun Cao,¹ Guang-Can Guo,¹ and Lixin He^{1,*}

¹Key Laboratory of Quantum Information, University of Science and Technology of China, Hefei, 230026, People's Republic of China

(Dated: April 24, 2019)

Cupric oxide is a unique magnetoferroelectric material with a transition temperature significantly higher than the boiling point of liquid nitrogen. However, the mechanism of high T_c multiferroicity in CuO remains puzzling. In this paper, we clarify the mechanism of high T_c multiferroicity in CuO using combined first-principles calculations and an effective Hamiltonian model. We find that CuO contains two magnetic sublattices, with strong intra-sublattice interactions and weakly frustrated inter-sublattice interactions, which may represent one of the main reasons for the high ordering temperature of the compound. The weak spin frustration leads to incommensurate spin excitations that dramatically enhance the entropy of the multiferroic phase and eventually stabilize that phase in CuO.

PACS numbers: 75.85.+t, 71.20.-b, 75.25.-j

Magnetoferroelectric materials, in which ferroelectricity is induced by magnetic ordering, have attracted intense interest [1, 2]. The strong magnetoelectric (ME) coupling in these materials opens a new path to the design of multifunctional devices that allow the control of charges by the application of magnetic fields or spins through applied voltages. However, nearly all current magnetoferroelectrics are strongly frustrated magnets [2], with very low ordering temperatures ($\sim 30 - 40$ K), several times lower than the temperatures expected from the strengths of their spin interactions. Low critical temperature is one of the major factors that limit the application of these important materials. Therefore, a new mechanism that allows high-temperature magnetoferroelectricity is highly desirable.

Recently, CuO has been found to be multiferroic at $T_c=230$ K, which is much higher than the critical temperatures of any other magnetoferroelectric materials [3]. CuO undergoes two successive magnetic phase transitions when it is cooled from room temperature to a temperature near zero. Neutron scattering experiments [4] have shown that at temperatures below $T_{N1}=213$ K, the spin structure is collinear antiferromagnetic (AF1) [see Fig. 1(a)]. Between T_{N1} and $T_{N2}=230$ K, the spin structure becomes non-collinear and slightly incommensurate (AF2) [see Fig. 1(b)], with a modulation vector of $\mathbf{Q} = (0.006, 0, 0.017)$. Elucidation of this unusual high-temperature multiferroic behavior may provide useful information in the search for novel room-temperature magnetoferroelectric materials. However, the mechanism that stabilizes the multiferroicity in CuO is still not understood, and it remains the subject of significant debate [5, 6].

In this work, we clarify the mechanism of high- T_c multiferroicity in CuO using combined first-principles calculations and simulations based on an effective Hamiltonian model. We find that CuO contains two magnetic sublattices, with strong intra-sublattice interactions and weakly

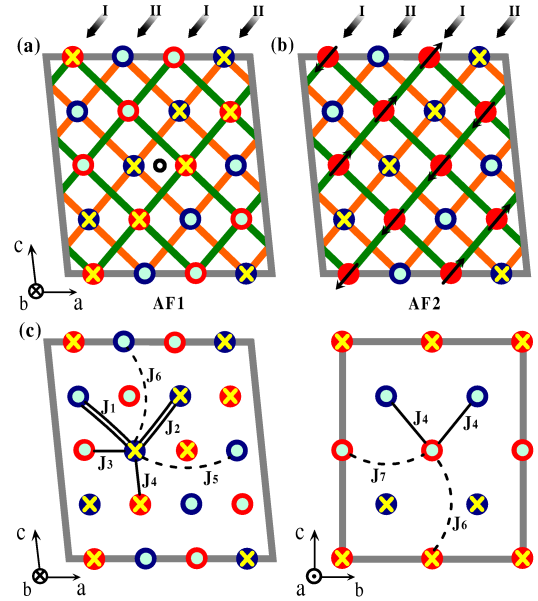


FIG. 1: Schematic sketch of the magnetic structures of (a) the collinear AF1 phase, and (b) the noncollinear AF2 phase. The black arrows, yellow crosses, and blue circles denote the spin directions associated with Cu ions. The black circle in (a) indicates an inversion center. (c) A sketch of superexchange interactions J_1 to J_7 . The single lines, double lines, and dashed lines represent the three types of exchange interactions between Cu ions.

frustrated inter-sublattice interactions, which might represent one of the main reasons that the compound exhibits a high ordering temperature. The weak spin frustration leads to incommensurate spin excitations that dramatically enhance the entropy of the AF2 phase and eventually stabilize the multiferroic phase. This mechanism is novel and differs from previously proposed mechanisms [5, 6]. This work suggests that high- T_c magnetoferroelectric materials can be sought in weakly frustrated magnets similar to CuO.

The crystal structure of CuO is monoclinic and contains four structural units per unit cell. The AF1 spin structure is composed of two anti-ferromagnetic (AFM) spin sublattices, shown in two different colors in Fig. 1 (a), in which Cu ions have the same b values in each sublattice. The spin chains along the $[10\bar{1}]$ direction are antiferromagnetic, and are labeled chain I and chain II for the two sublattices, whereas the chains along the $[101]$ direction are ferromagnetic. In the AF1 phase, all spins are aligned in the b direction, whereas in the AF2 phase, chain II rotates perpendicularly to chain I.

We perform ab initio calculations on CuO, with non-collinear spin-polarized local density approximation (LSDA) implemented in the Vienna ab initio simulations package (VASP) [7, 8]. The on-site Coulomb interactions $U=7.5$ eV are included for Cu ions in a rotationally invariant scheme introduced by Liechtenstein et. al. [9]. The spin-orbit coupling is considered in the calculation unless otherwise noted. To accommodate the spin structures, we use a $2\times 1\times 2$ CuO supercell that contains 32 atoms. For the AF2 structure, we neglect the small incommensurate component of the spin structure [i.e., we set $\mathbf{Q} = (0, 0, 0)$], and rotate the spin directions of chain II 90° , so that it lies in the ac plane. The spins form cycloidal spirals along both the a and c axes in the AF2 phase. The incommensurate component of the magnetic modulation vector \mathbf{Q} is extremely small, and it should not affect the calculated electric polarization because $P \propto \mathbf{S}_i \times \mathbf{S}_j$ [10]. More details of the first-principles calculations can be found in the supplementary materials.

We first determine the crystal structure of CuO under the AF1 spin configuration. The room temperature crystal structure is monoclinic and of space group $C2/c$, with inversion symmetry. However, the magnetic structure of the AF1 phase only has $P2_1/c$ symmetry. Therefore, after relaxation, the crystal structure is also reduced to $P2_1/c$ symmetry because of “exchange restriction” effects [11]. Further analyses [11] show that the Cu and O ions deviate from their high symmetry sites by approximately 10^{-3} Å. This distorted structure preserves the inversion symmetry; therefore it has no net polarization. The inversion center is shown in Fig. 1(a). An inversion operation about the inversion center changes spin chain I to chain II.

We then fix the spin orientations to the AF2 configuration and relax the crystal structure again to obtain the crystal structure of the AF2 phase. The calculated total energy of the AF2 phase is greater than that of the AF1 phase by approximately 0.33 meV per atom, which is consistent with experiments that have shown the AF2 phase to appear at a higher temperature than that at which the AF1 phase appears [4, 12, 13]. Before structural relaxation, the total energy of the AF2 phase is approximately 0.08 meV per atom higher than that of the AF1 phase. This energy difference is primarily at-

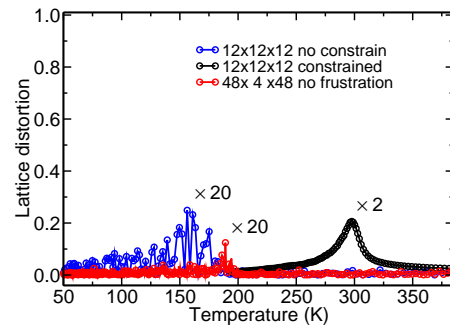


FIG. 2: The polar lattice distortions u_2 as functions of temperature. The maximum value of the lattice distortion is set to 1. Blue curve: the result of the $12\times 12\times 12$ lattice. Red curve: the result of the $48\times 4\times 48$ lattice without frustrated spin interactions. Black curve: the result of the $12\times 12\times 12$ lattice, with the spins are constrained in 4 perpendicular directions. The lattice distortion values are amplified by factors of 20, or 2 as indicated in the figure.

tributed to the spin anisotropy energy, which can be observed when the spin-orbit coupling is turned off, which reduced the energy difference between the two phases to 0.03 meV per atom. The remaining difference of 0.25 meV per atom exists because the ionic distortion in the AF1 phase is substantially larger than that in the AF2 phase, as shown below.

The AF2 spin structure exhibits $P2_1$ space group symmetry, to which the rotation of spin chain II does not give inversion symmetry, as can be seen in Fig. 1(b). The crystal structure is distorted by the Dzyaloshinskii-Moriya (DM) interaction [14–16], which breaks the inversion symmetry. When compared with the high symmetry structure, all the oxygen ions are shifted in the $-b$ direction by approximately 7×10^{-5} Å, whereas all Cu ions are shifted in the $+b$ direction by a similar amount. The ionic distortion in the AF2 phase is approximately two orders of magnitude smaller than that driven by the “exchange restriction” effects in the AF1 phase.

Next, we calculate the electric polarization using the Berry-phase theory of polarization [17]. The calculated total polarization is approximately $90 \mu\text{C m}^{-2}$ in the $-b$ direction, which is somewhat smaller in magnitude than the experimental value of $160 \mu\text{C m}^{-2}$ along the b axis. The agreement between the theoretical calculations and experimental values is reasonable, given that the current functionals are not adequate to treat the subtle correlation effects in magnetoelectric materials [18].

In magnetoelectric materials, the transition temperatures are predominantly determined by the magnetic exchange interactions [3]. We extract the superexchange interactions J_s of CuO using a Heisenberg model, $H_M = -\sum_{ij} J_{ij} \mathbf{S}_i \cdot \mathbf{S}_j - \sum_i (\mathbf{K} \cdot \mathbf{S}_i)^2$ from the calculated total energies of the different spin configurations in the symmetrized $C2/c$ crystal structure with SOC. \mathbf{K} is the anisotropic energy due to SOC. There are seven J values

in total, which are shown in Fig. 1(c). Among them, J_1 is the exchange interaction between nearest-neighbor (NN) Cu atoms along the $[10\bar{1}]$ direction, J_2 is the interaction between NN Cu atoms along the $[011]$ direction, J_7 is the interaction between the NN spins of the same sublattice along the b direction, and J_3 and J_4 are the inter-sublattice exchange interactions. The fitted value of $J_1 = -51$ meV is in good agreement with the value determined from neutron scattering experiments, $J = 67 \pm 20$ meV [4]. The fitted value of $J_2 = 8.6$ meV, is only approximately 1/6 the value of $|J_1|$, which is consistent with the quasi-1D model [19], and the fitted value of $J_7 = 9.87$ meV. The fitted inter-sublattice coupling value $J_3 = 4.9$ meV and $J_4 = 7$ meV, are weak because the Cu-O-Cu bond angles are close to 90° for these two J s [19]. In the AF1 and AF2 phases, symmetry causes additional mutual cancellation of J_3 and J_4 ; therefore, the energy cost of chain II rotation is low, as was discussed in the previous paragraph. We also calculate the next-nearest-neighbor (NNN) interactions, J_5 and J_6 . We find that J_5 and J_6 are highly asymmetric. Interaction J_5 is significant, with a value of -12 meV, whereas J_6 is only 2.1 meV. These values agree well with those of Filippetti and Fiorentini [20].

The intra-sub-lattice interactions J_1 , J_2 and J_7 essentially determine the ground state spin structure, AF1. The J_5 NNN interactions further favors the antiferromagnetic spin chain along the $[10\bar{1}]$ direction, whereas, J_6 only adds a small frustration to this configuration. The major competing interactions are those of the inter-sublattice interactions, J_3 and J_4 . The weak incommensurateness of the spin spiral caused by the frustrated exchange interactions J_3 , J_4 is consistent with that effect in this material because the spin competition is small. We calculate the ordering temperature of the Heisenberg model by a Monte Carlo simulation, in which all exchange interactions are forced to be ferromagnetic and we obtain $T_c = 311$ K [21]. This temperature is only about 1.5 times greater than the T_c value of the AF1 phase, (In RMn_2O_5 [22], the ratio is approximately 3 - 4.), which also indicates that the spin frustration is weak in CuO. The lack of strong competing interactions in this compound may explain the high spin-ordering temperature of CuO.

To study the multiferroic phases of CuO, we simulate the full Hamiltonian model with spin-lattice interactions, $H = H_{\text{ph}} + H_{\text{M}} + H_{\text{I}} + H_{\text{DM}}$, where,

$$H_{\text{ph}} = E_0 + \sum_k \frac{1}{2} m_1 \omega_1^2 u_1^2(k) + \frac{1}{2} m_2 \omega_2^2 u_2^2(k), \quad (1)$$

$$H_{\text{I}} = \sum_{i,j} \sum_{k,\lambda} J'_{ij} u_1(k) \mathbf{S}_i \cdot \mathbf{S}_j, \quad (2)$$

$$H_{\text{DM}} = \sum_{i,l>0} D[u_2(i) \hat{\mathbf{b}} \times \mathbf{e}_{i,i+l}] \cdot (\mathbf{S}_i \times \mathbf{S}_{i+l}). \quad (3)$$

Here E_0 is the energy of the high-symmetry structure without magnetic interactions. The lattice distortions in

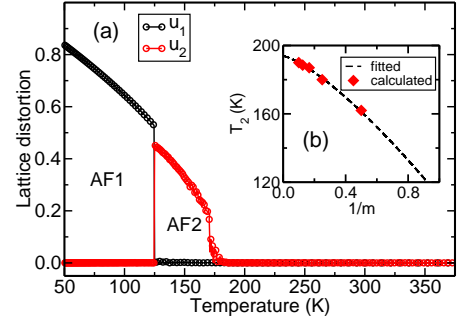


FIG. 3: (a) The lattice distortions u_1 (black) and u_2 as functions of temperature. The maximum value of the lattice distortion is set to 1. (b) The transition temperature T_2 scaling with different simulation size m .

the AF1 and AF2 phases are characterized by the non-polar modes $u_1(k)$, and the polar modes $u_2(k)$, of the k -th unit cell, respectively, and m_1 (m_2) and ω_1 (ω_2) are the reduced mass and frequency of the non-polar modes (polar modes), respectively. For simplicity, we neglect the phonon dispersion in the simulation, which has little effect on the results [22]. H_{I} is the isotropic spin-lattice interaction caused by exchange restriction effects. In CuO, only J'_3 and J'_4 are involved in the nonpolar lattice distortion, and the other J 's cancel each other by symmetry. H_{DM} is the DM interaction term, which sums over the nearest neighbor spin l along the a and c axes, where $\hat{\mathbf{b}}$ is the unit vector along the b (polar) axis and $\mathbf{e}_{i,i+l}$ is a unit vector joining the i -th and the $i+l$ -th Cu atoms. Unlike the model in Ref. [5], our model explicitly includes the lattice degree of freedom, especially the non-polar modes, which are missing in the model of Ref. [5].

For simplicity, we redefine u_1 (u_2) to be a dimensionless parameters that takes the value of unity at the low-symmetry state of the AF1 (AF2) phase, and we assign spin moments $|\mathbf{S}_i| = 1.0$. All parameters in the model can be obtained by fitting to the total energies of the first-principles calculations [22]. We use $J'_3 = J'_4 = 0.8163$ meV, which is approximately 1.5 times greater the values obtained by first-principles calculations [23]. To obtain the correct ground state, we reduce the values to $J_3 = 2.45$ meV, and $J_4 = 3.5$ meV, which are approximately half of the fitted values. $m_1 \omega_1^2 = 0.4$, $m_2 \omega_2^2 = 0.49D$. $D_c = 0.8723$ meV is the critical value at which the energies of AF1 and AF2 phases are degenerate.

We simulate the effective Hamiltonian model in the temperature range from 29 to 387 K, using a replica-exchange Monte Carlo (MC) method [22]. We perform the MC simulations on the $n \times m \times n$ lattices ($n=12-72$, $m=2-12$) with periodic boundary conditions. The electric polarization $P = \langle u_2 \rangle$. Typical simulation results for the $n=12$ lattice are shown in Fig. 2. There is no stable AF2 phase, even with a large DM interaction, $D=0.5D_c$. If we *artificially* constrain the spin to only four possible directions at 90° , as was done by Giovannetti et al. [5],

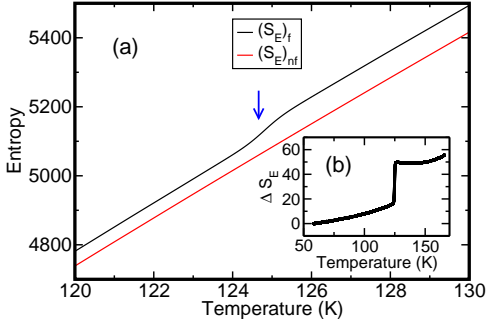


FIG. 4: (a) The entropies as functions of the temperature of the $48 \times 4 \times 48$ lattice with (black line) and without (red line) frustrated spin interactions. (b) The entropy difference between the systems with/without frustrated spin interactions.

we obtain a *weak* AF2 phase at approximately 300 K, as shown in Fig. 2, that is similar to the one obtained by Giovannetti et al. [5]. The above results suggest that the DM interaction alone cannot stabilize the AF2 phase in CuO.

Surprisingly, if the simulation lattice size is increased to $n > 32$, a well defined AF2 phase is obtained. The simulation results of a $48 \times 4 \times 48$ lattice with a small $D = 0.066 D_c$ are presented in Fig. 3(a). A PE to FE transition clearly occurs near $T_2 = 180$ K. At $T_1 = 125$ K, the polarization suddenly drops to zero, accompanied by the appearance of the non-polar lattice distortion, which indicates that the system enters the AF1 phase. This result is in excellent agreement with experiments. Fourier analyses of the spin structures [22] also confirm the above results. A finite size scaling for T_2 with m gives $T_2 = 192$ K as $1/m$ approaches zero [see Fig. 3(b)], which slightly underestimates the experimental value of $T_2 = 230$ K [3].

It is initially surprising that the AF2 phase is not stable in the small simulation lattice but survives in the large simulation lattice. Fourier analyses of the spin structures suggest that, in the $n = 48$ lattices, many incommensurate spin components are present, which are forbidden in the small (e.g., $n = 12$) lattices. The incommensurate spin components are generally known to arise from the frustrated spin interactions, which suggests that the small spin frustration might play an important role in stabilizing the AF2 phase. We then perform the simulations using the $48 \times 4 \times 48$ lattice, but set the frustrated spin interactions to zero, i.e., $J_3 = J_4 = J_6 = 0$. The results are shown in Fig. 2. Remarkably, the results are very similar to those obtained for the $n = 12$ lattice, and no stable AF2 phase is found. This result further confirms the assumption that the weak spin frustration is essential to stabilize the AF2 phase, and contradicts to previous conclusions [5, 6].

To understand why the weak incommensurate spin components can stabilize the AF2 phase, we calculate the entropy of the system of as a function of the temperature

using a multi-histogram reweighting technique[24]. The entropies of the $48 \times 4 \times 48$ lattice with or without spin frustration are compared in Fig. 4. The entropy of the non-frustrated system increases smoothly as temperature increases from 120 K to 130 K. The entropy of the $n = 12$ lattices with frustrated interactions (not shown) exhibits a similar temperature dependence. In contrast, an obvious entropy jump occurs near $T_1 = 125$ K in the $48 \times 4 \times 48$ lattice with spin frustration. This increase can be seen more clearly in Fig. 4 (b), which depicts the difference of the system entropies with and without spin frustrations in the temperature range 50 -160 K. Therefore, we conclude that the incommensurate spin excitations caused by the spin frustration greatly enhances the entropy of the system in the AF2 phase and stabilizes the phase.

To explore the role of the DM interaction in the phase transitions, we tune the DM interaction strength D from zero to D_c . In the range of $D < D_c$, transitions from the PM-PE phase to the AF2-FE phase to the AF1-PE phase are always present. As D increases, the temperature range of the AF2 phase also increases. When $D > D_c$, only the transition from the PM-PE phase to AF2-FE phase exist, and there is no AF1 phase [5]. Interestingly, when we set $D = 0$, we still obtain a stable AF2-like incommensurate phase, but with it has no net electric polarization because there is no unique polarization axis in this case. The DM interaction that breaks the rotational symmetry of the nearly degenerate spin structures in the AF2 phase and generates the polarization axis [5]. However, in the case of a strong magnetic anisotropy, electric polarization is also possible.

Understanding the mechanism of the multiferroicity in CuO provides important guidance in the search for new high T_c magnetoelectric materials. We found that CuO contains two magnetic sublattices, with strong intra-sublattice interactions and weakly frustrated inter-sublattice interactions, which may represent one of the main reasons that the compound has a high ordering temperature. Monte Carlo simulations suggest that the incommensurate spin excitations, caused by the weak frustrated interactions dramatically enhance the entropy of the multiferroic AF2 phase, and they eventually stabilizes the phase. The DM interaction break the magnetic rotational symmetry, which causes lattice distortion and lead to electric polarization in the AF2 phase. This mechanism is distinct from previously proposed mechanisms [5, 6] for CuO. One of the fascinating features of magnetoferroelectric materials is their rich phase diagrams, which arises from the competing interactions in these materials. However, few reports on the mechanism of these phase transitions at the microscopic level have been published. The methods developed in this work may be useful in elucidating the complex magnetoferroelectric phase transitions in general magnetoferroelectric materials.

LH acknowledges the support of the Chinese National Fundamental Research Program 2011CB921200, the Na-

tional Natural Science Funds for Distinguished Young Scholars, and the Fundamental Research Funds for the Central Universities No. WK2470000006.

* Electronic address: helx@ustc.edu.cn

- [1] M. Fiebig, J. Phys. D: Appl. Phys. **38**, R123 (2005).
- [2] S.-W. Cheong and M. Mostovoy, Nature Materials **6**, 13 (2007).
- [3] T. Kimura, Y. Sekio, H. Nakamura, T. Siegrist, and A. P. Ramirez, Nature Materials **7**, 291 (2008).
- [4] B. X. Yang, T. R. Thurston, J. M. Tranquada, and G. Shirane, Phys. Rev. B **39**, 4343 (1989).
- [5] G. Giovannetti, S. Kumar, A. Stroppa, J. van den Brink, S. Picozzi, and J. Lorenzana, Phys. Rev. Lett. **106**, 026401 (2011).
- [6] P. Tolédano, N. Leo, D. D. Khalyavin, L. C. Chapon, T. Hoffmann, D. Meier, and M. Fiebig, Phys. Rev. Lett. **106**, 257601 (2011).
- [7] G. Kresse and J. Hafner, Phys. Rev. B **47**, RC558 (1993).
- [8] G. Kresse and J. Furthmüller, Phys. Rev. B **54**, 11169 (1996).
- [9] V. I. Anisimov, J. Zaanen, and O. K. Andersen, Phys. Rev. B **44**, 943 (1991).
- [10] M. Mostovoy, Phys. Rev. Lett. **96**, 067601 (2006).
- [11] C. Wang, G.-C. Guo, and L. He, Phys. Rev. B **77**, 134113 (2008).
- [12] P. J. Brown, T. Chattopadhyay, J. B. Forsyth, and V. Nunez, J. Phys.: Condens. Matter **3**, 4281 (1991).
- [13] M. Ain, A. Menelle, B. M. Wanklyn, and E. F. Bertaut, J. Phys.: Condens. Matter **4**, 5327 (1992).
- [14] I. E. Dzyaloshinskii, Sov. Phys. JETP **19**, 960 (1964).
- [15] T. Moriya, Phys. Rev. **120**, 91 (1960).
- [16] I. A. Sergienko and E. Dagotto, Phys. Rev. B **73**, 094434 (2006).
- [17] R. D. King-Smith and D. Vanderbilt, Phys. Rev. B **47**, 1651 (1993).
- [18] A. S. Moskvina and S.-L. Drechsler, Phys. Rev. B **78**, 024102 (2008).
- [19] T. Shimizu, T. Matsumoto, A. Goto, T. V. ChandrasekharRao, K. Yoshimura, and K. Kosuge, Phys. Rev. B **68**, 224433 (2003).
- [20] A. Filippetti and V. Fiorentini, Phys. Rev. Lett. **95**, 086405 (2005).
- [21] The simulations are done in a $12 \times 12 \times 12$ lattice, with magnetic interactions only.
- [22] K. Cao, G.-C. Guo, D. Vanderbilt, and L. He, Phys. Rev. Lett. **103**, 257201 (2009).
- [23] We adjust the parameters of the model Hamiltonian slightly from the fitted values, because first-principle calculations may not be accurate enough in this situation with subtle competing interactions.
- [24] A. M. Ferrenberg and R. H. Swendsen, Phys. Rev. Lett. **63**, 1195 (1989).